

DESIGN FEATURES OF THE INPUT COUPLER FOR THE DTL

F. Naito, T. Kato, Y. Morozumi, E. Takasaki, Y. Takeuchi
and Y. Yamazaki
National laboratory for High Energy Physics, KEK
1-1 Oho, Tsukuba-shi, Ibaraki-ken, 305 Japan

Abstract

An rf input coupler for a drift-tube linac was designed and studied with the computer codes and the low-power models. It comprises four parts; a door-knob transition, an rf window of the ceramic disk, a short transformer of the coaxial waveguide and an rf loop coupler. The reliability of the design aided with computer codes was confirmed with the model test.

Introduction

A 432-MHz drift-tube linac (DTL) that accelerates the H⁺ ions to 150 MeV will be constructed as a part of 1-GeV injector linac for a ring accelerator of the Japanese Hadron Project (JHP)¹. The tank of the DTL is driven with an rf power of 0.92 MW and a duty factor of 3% (600-msec pulse length and 50-Hz repetition rate). As a high-power 5.4-MeV DTL for a low energy beam test is under construction, an input coupler for the DTL is prepared for the high-power and beam tests.

An rf input coupler is one of the most important parts of a linac for the stable operation. Since a number of troubles during the operation of a linac have been related to an input coupler, the reliability of a linac system is largely dependent on that of an input coupler.

The output coupler of the 508-MHz klystron that feeds an rf power into the cavity of the TRISTAN works with high stability under the operation of 1.2 MW and 100% duty factor², being 1.3 times and 33 times as large as those of the DTL, respectively. Its design should be useful for an input coupler of the 432-MHz DTL.

Figure 1 shows the cross section of the output coupler of the 508-MHz klystron². It is composed of three transition sections.

(1) The first section is the transformer between the coaxial wave guide of the WX77D and that of the WX152D. This junction also works as a shield of the rf window and a supporting disk from an irradiation caused with the beam in the cavity.

(2) The second section is a coaxial wave guide of WX152D with a ceramic-disk window. Inside- and outside-diameters of the rf window are 166 and 38 mm, respectively; the thickness is 10 mm. A relative dielectric constant of the ceramic disk is about 9. The impedance is matched with the choke structure.

(3) The third section is the door-knob transition between the coaxial wave guides of the WX152D and the rectangular wave guide of the WR1500.

Since the operational frequency 432 MHz for the DTL is different from the TRISTAN, the dimensions of each transformer must be readjusted in order to match the impedance at 432 MHz. When it is not easy to make a reliable equivalent circuit for a transformer, the transition section is designed with a number of "cut and try" in the models. In this paper, the computer codes, SUPERFISH³ and MAFLA⁴, are applied to the design of the transition section owing to the following advantages.

- (1) The application saves the number of the "cut and try."
- (2) Since the field distribution is illustrated, it is possible to improve the design in order to avoid a local strong electric field that gives rise to the break down.

The design principle for the application of the computer codes is summarized in the next section. The details of the design for each transition section are described thereafter.

The design principle of the transformer section on the basis of the computer codes

With the computer codes, SUPERFISH and MAFLA, we can obtain the standing-wave solution of a cavity under a given boundary condition. Since the traveling wave can be described in terms of a linear combination of two independent standing waves, these computer codes can also be applied to the traveling wave problems, as follows.^{5,6}

- 1) Introduce the boundary planes S₁ and S₂ in the port-1 and port-2,

respectively, as shown in Fig. 2. Calculate the resonant frequencies of the transformer bounded with S₁ and S₂ under two independent cases C₁ and C₂ of the boundary conditions; denote the resonant frequencies of the cases C₁ and C₂ by f₁ and f₂, respectively. For example, the case C₁ may imply short boundary conditions for both the S₁ and S₂, while the case C₂ may imply open conditions for both. It is noted that other cases can be chosen as far as the two cases are independent of each other.

2) Adjust one of the positions of the S₁ and S₂, for example S₁, until f₁ becomes equal to the operational frequency f₀ and denotes the adjusted position by P₁₁. Also, readjust the position of the S₁, until f₂=f₀ is obtained and denote it by P₁₂.

3) If the transformer is matched, the position P₁₁ is the same as P₁₂.

4) In the mismatched case, the reflection coefficient can be estimated for the difference between P₁₁ and P₁₂.
The procedure described above is applied to the design of a transformer. The input geometry of the transformer is optimized so that it meets the requirement of situation 3). The procedure will be particularly useful in the case that no reliable equivalent circuit exists. The code SUPERFISH is applied to the axially symmetric case and the code MAFLA for the asymmetric case.

The transformer between the coaxial wave guides

A short transformer is sufficient to match the two coaxial lines that have the same impedance but different diameters⁷. Since it is difficult to calculate the matched condition of the transformer with an equivalent circuit, the above-mentioned procedure with the code SUPERFISH was applied to the design of the transformer between the coaxial waveguide of WX77D and that of WX152D. Figure 3 shows the configuration of the transformer. The total length of the transformer is held fixed to 44.7 mm during calculation. A variable parameter is the length L₁ of the taper section of an inside cylinder shown in Fig. 3. Figure 4 shows the electric field patterns calculated with SUPERFISH for two boundary conditions. In Fig. 4-a both planes of S₁ and S₂ have the open boundary condition, while the short boundary condition in Fig. 4-b. The former corresponds to the condition of the C₁ and the latter corresponds to that of the C₂. The position of S₁ and S₂ are optimized in order to adjust a resonant frequency to the f₀.

The condition f₁=f₂=f₀(=432 MHz) was obtained with the L₁ of 30.7 mm. Figure 5 shows the dependences of the resonant frequencies' f₁ and f₂ on the parameter L₁. The measured VSWR of the model transformer designed on the basis of this calculation was less than 1.05 at 432 MHz, supporting the reliability of the design method.

The rf window of the ceramic disk

An rf window of the ceramic disk is installed in the coaxial waveguide in order to hold the vacuum in the DTL. At first, we have studied the rf window with the same size as that of 508 MHz klystron. The electric field pattern of the rf window with the choke structure was calculated with SUPERFISH and is shown in Fig. 6. Since it has a mirror symmetry on the center of the rf window, half of the structure was used for the calculation, holding virtual boundary plane S1 fixed in the middle of the rf window. The boundary condition of the plane S1 is open, while that of S₂ short, for the case of C₁, as seen in Fig. 6-a. The C₂ has the opposite boundary condition to the C₁, as shown in Fig. 6-b.

Variable parameters are the thickness t_i of the inside choke and the depth l_i of the inside and the outside chokes. There are two solutions. One is given with t_i=6 mm and l_i=43 mm. The other is given with t_i=5 mm and l_i=40 mm. The electric field pattern of the latter case is shown in Fig. 6. The frequencies were adjusted with changing the t_i keeping l_i constant. The frequency f₁ on the boundary condition C₁ is independent of the length l_i because the electric field does not exist in the choke.

One of the advantages of the choke coupling is that outlets of cooling air are located in the choke where no electric field exists.

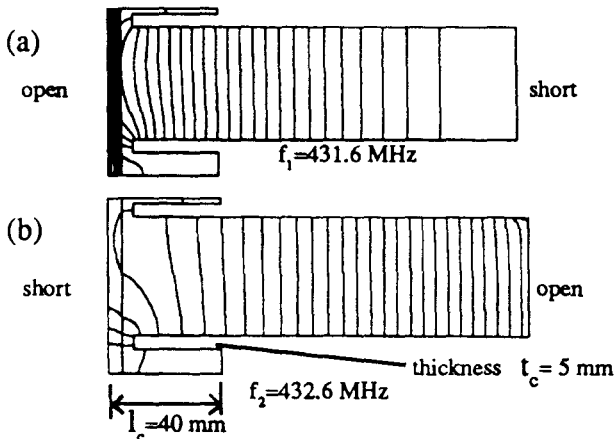


Fig. 6. Electric field pattern for the rf window of the choke type calculated with SUPERFISH.

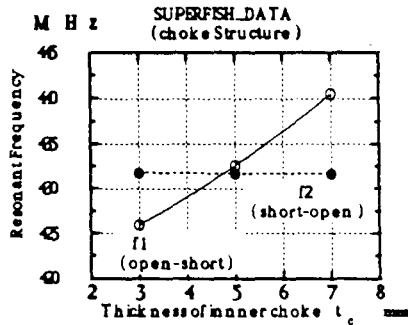


Fig. 7. Resonant frequencies f_1 (open-short) and f_2 (short-open) of the rf window of the choke type.

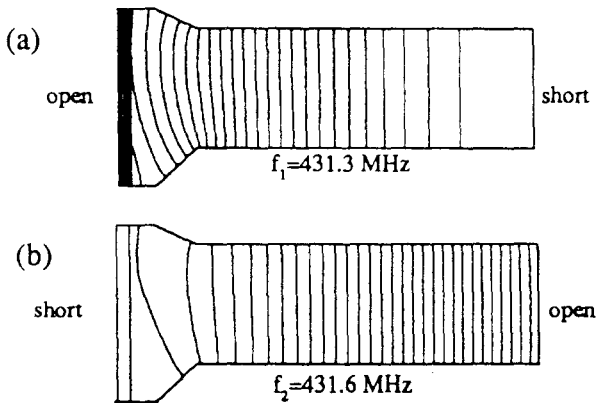


Fig. 8. Electric field pattern of the rf window of under/over cut type calculated with SUPERFISH.

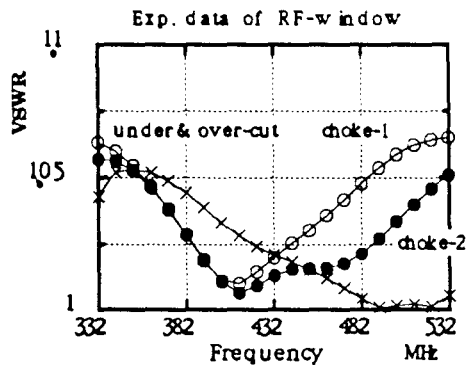


Fig. 9. Experimental data of VSWR for a low power model of the rf windows.

choke-1; $t_c=6$ mm, $l_c=43$ mm
choke-2; $t_c=5$ mm, $l_c=40$ mm

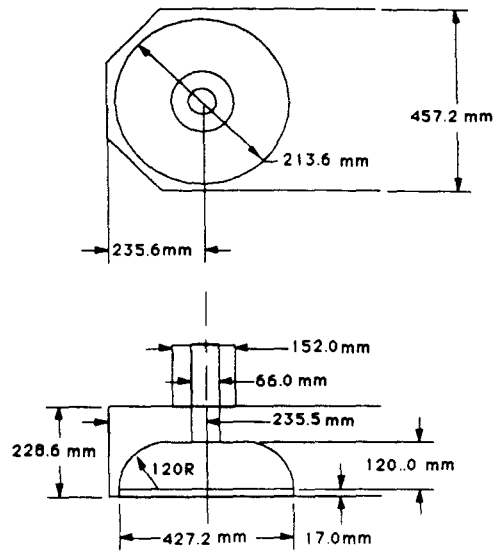


Fig. 10. Dimension of the 432 MHz door-knob transition.

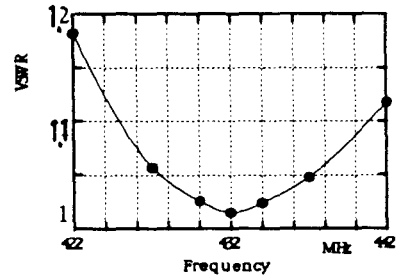


Fig. 11. Experimental data of VSWR for a low power model of the door-knob transition.

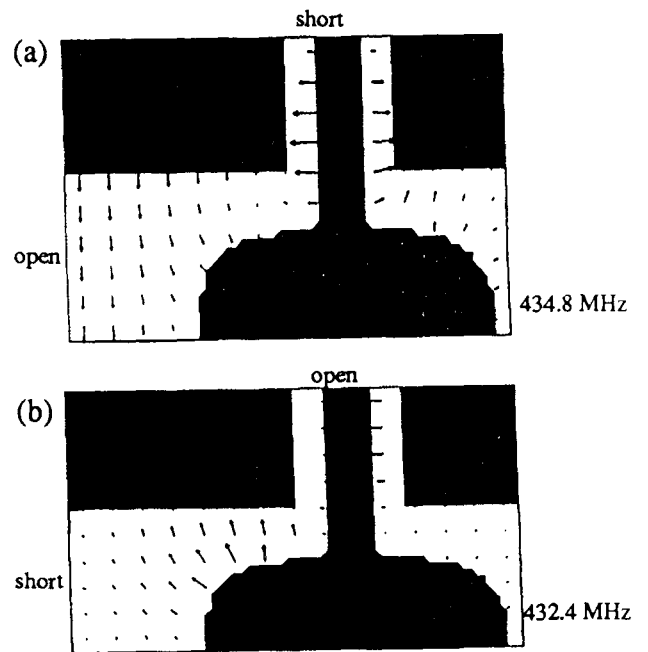


Fig. 12. Electric field patterns of the door-knob transition calculated with MAFLA.

Therefore, the size and shape of the air outlet can be easily designed. The disadvantages are that the structure becomes complicate and that the electric field normal to the rf window is induced. The electric field normal to the rf window gives rise to the multipactoring that results in the break down. Thus, the gap size between the ceramic and the head of the choke should be determined carefully in order to avoid the break down.

The impedance matching of an rf window can also be obtained with the structure of an under- and/or an over-cut of the waveguide. The rf window of the under-cut structure is in operation for the higher-mode damper of the accelerating cavity of TRISTAN[®]. The rf window with both over- and under-cuttings was designed by referring to the shape of the higher-order mode damper. It can be seen from the electric field pattern shown in Fig. 8 that the direction of the electric field is almost parallel to the rf window. This is more advantageous than the choke structure regarding the suppression of multipactoring and a local heating. However, the air outlets are located on the slope of under- and over-cutting area where the electric field exists. Thus, special care will be necessary to determine the size and the shape of the outlet, considering the cooling of the rf window and a field disturbance.

Figure 9 shows the experimental data of VSWR of the models for the rf window, designed with the present procedure. The VSWR for the frequency ranging from 382 to 482 MHz is less than 1.05 for all the structures studied. This data also supports the reliability of the design with the present procedure.

The door-knob transformer

The door-knob transformer was designed with the standard "cut and try" method. In principle the computer code MAFIA can be applied to the design of the door-knob transformer. However, the available mesh number of MAFIA was not sufficiently large for the design.

The basic dimension was determined with a scaling of the size of the coupler of 508-MHz klystron. The tuning parameters were the position of the moving short plane and the thickness of the spacer between the door-knob and the wave guide. Figure 10 shows the dimension of the door knob. The measured VSWR of the door-knob model is shown in Fig. 11.

Since the maximum number of the meshes in MAFIA has recently been increased to 10⁶ in KEK, we applied MAFIA to the door-knob study. The electric field pattern is shown in Fig. 12. It can be seen that the field pattern changes from a rectangular waveguide mode (TE₀₁) to a coaxial waveguide mode (TEM) smoothly, leaving no strong electric field localized.

Conclusions

The input coupler of the 432 MHz DTL for the Japanese Hadron Project was designed. It is confirmed that the impedance matching of the transformer could be obtained with the SUPERFISH-aided design. The door-knob transition was designed with the model study. Its field pattern was checked with the code MAFIA.

Acknowledgment

The authors are extremely grateful for the advice offered by Prof. H. Baba.

References

1. T. Kato, Y. Yamazaki and M. Kihara, Proc. 2nd Int. Sym. on Advanced Nucl. Energy Research, JAERI, Japan, (1990), 177.
2. S. Isagawa, et al., Proc. IEEE Part. Accel. Conf., Washington D.C., (1987) 16
3. K. Halbach and R. F. Holsinger, Part. Accel. 7 (1976) 213
4. T. Weiland, Part. Accel., 15 (1984) 245
5. J. C. Slater, "Microwave Electronics", D. Van Norstrand, (1950)
6. Y. Yamazaki, a note of the "Proton Linac seminar," in KEK, unpublished, 1990
7. G. L. Ragan, "Microwave Transmission Circuit," MIT, Rad. Lab. Ser.9 (1948) 305
8. Y. Morozumi, T. Higo and Y. Yamazaki, Part. Accel., 29 (1990) 85

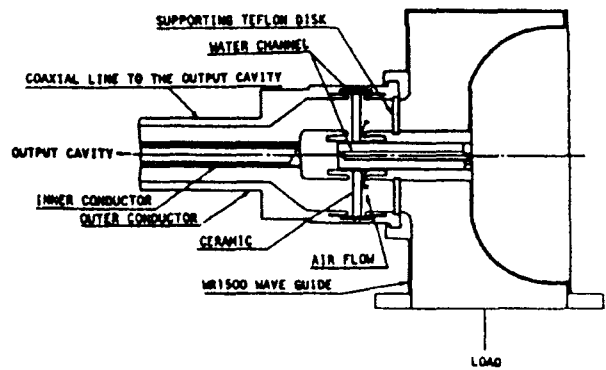


Fig. 1. Cross section of the output coupler of 508 MHz klystron².

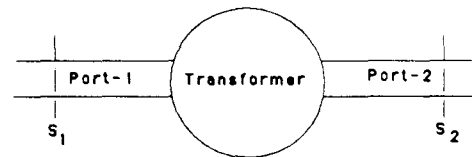


Fig. 2. Model of two ports transformer.

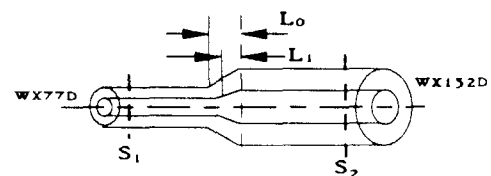


Fig. 3. Configuration of transformer for joining two coaxial lines.

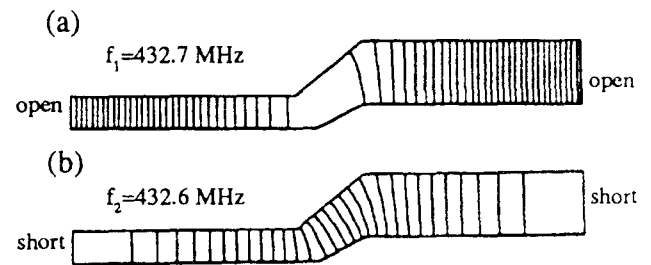


Fig. 4. Electric field patterns of the transformer calculated with SUPERFISH. ($L_0=44.7$ mm, $L_1=30.7$ mm)

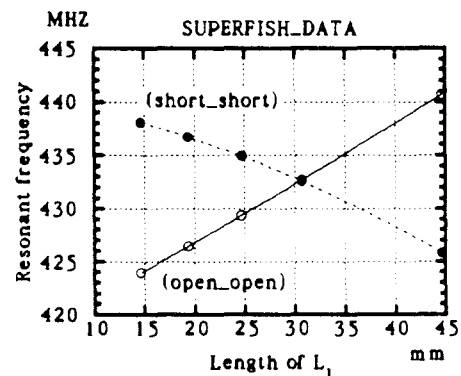


Fig. 5. Resonant frequencies f_1 (open-open) and f_2 (short-short) of the coaxial line transformer.